ELSEVIER

European Journal of Pharmacology 314 (1996) 357–364

ejp

Effects of charybdotoxin on K^+ channel (Kv1.2) deactivation and inactivation kinetics

Leslie K. Sprunger [a,1], Nancy J. Stewig [b], Scott M. O'Grady [a,b,*]

[a] *Department of Physiology, University of Minnesota, St. Paul, MN 55108, USA*
[b] *Department of Animal Science, University of Minnesota, St. Paul, MN 55108, USA*

Received 1 July 1996; accepted 9 July 1996

Abstract

Of particular interest for voltage-gated K^+ channels are the effects of membrane voltage and pharmacologic agents on channel kinetics. We have characterized in detail properties of a Kv1.2 channel expressed in oocytes as the basis for investigation of its structure-function relationships. This channel exhibited a voltage-dependent rate of activation with a $V_{1/2}$ of −21 mV. Voltage-dependent steady-state inactivation overlapped the activation curve with half-maximal inactivation occurring at −22 mV. Dendrotoxin inhibited channel activation with an IC_{50} of 8.6 nM at +35 mV. Charybdotoxin also blocked this K^+ channel (IC_{50} = 5.6 nM). While dendrotoxin block was not affected by channel activation, charybdotoxin exhibited additional accumulation of block following activation, which was relieved with a time constant of 0.5 s upon repolarization of the membrane. The deactivation of this channel was accelerated in the presence of charybdotoxin while not significantly affected by dendrotoxin.

Keywords: Charybdotoxin; Dendrotoxin; Voltage dependence; Channel kinetics; Inactivation; Deactivation

1. Introduction

Our understanding of the structure-function relationship of voltage-gated K^+ channels has advanced rapidly in the last decade with the cloning of many different K^+ channel genes and their subsequent expression in various in vitro systems (for reviews, see Brown, 1993; Andersen and Koeppe, 1992; Pongs, 1992, 1993). Included in the family of voltage-gated K^+ channels is the group classically referred to as delayed rectifiers. As indicated by the name, these channels open with a significant delay relative to sodium channels after a change in membrane potential, with 95% rise times typically greater than 10 ms. The degree of rectification exhibited by members of this group is variable, reflecting both Goldman rectification and intrinsic channel properties. The physiological role of delayed rectifiers also varies depending on cell type. In non-excitable cells, they are likely to be involved in volume regulation and may be important in offsetting membrane depolarization produced by electrogenic anion efflux in epithelial cells (Cooper et al., 1990; O'Grady et al., 1991). There is some evidence to show the involvement of delayed rectifiers in the activation of lymphocytes (Brent et al., 1990; Verheugen et al., 1994; Leonard et al., 1992). In cardiac tissue, the delayed rectifier is critical in determining the duration of the plateau phase of the action potential and is, therefore, a major determinant of cardiac rate and rhythm (for a review, see Katz, 1993).

With respect to channel modifiers and blockers, delayed rectifiers exhibit considerable diversity. They are generally susceptible to block by extracellular Ba^{2+} in a voltage-dependent manner. The IC_{50} for extracellular tetraethylammonium can vary by two orders of magnitude or more for different delayed rectifiers. Charybdotoxin, representative of a family of venom toxins, blocks some delayed rectifiers at nanomolar concentrations while others are virtually insensitive. Similar observations have been reported for the structurally related snake-venom toxin, dendrotoxin. The stoichiometry of toxin binding is one-to-one (Miller, 1988; MacKinnon and Miller, 1988; Giangiacomo et al., 1992) and the kinetics of binding are compatible with a simple bimolecular reaction model (Gross et al.,

* Corresponding author. Tel.: (1-612) 624-3767; Fax: (1-612) 625-2743.
[1] Current address: Department of Human Genetics, University of Michigan, Ann Arbor, MI 48109, USA.

PII S0014-2999(96)00556-0

1994). The receptor for charybdotoxin has been localized to the S5-S6 linker in Kv1 and Kv2 channels, with specific amino-acid residues having been identified which most strongly affect toxin sensitivity (Goldstein and Miller, 1992; Goldstein et al., 1994; Gross et al., 1994). In addition to furthering our understanding of the nature of channel-toxin interaction, detailed studies of blocker pharmacology, kinetics and comparisons of primary structure between channels continue to provide valuable insight into intrinsic channel properties and how these properties may be determined by structure.

A delayed rectifier channel cloned from rat atrium was initially described and named RAK by Paulmichl et al. (1991); according to the current classification scheme, it is a Kv1.2 type voltage-gated K^+ channel (Chandy, 1991) and will be referred to in this paper as rKv1.2. While several properties of Kv1.2 channels expressed in mammalian cell lines have been reported (Grissmer et al., 1994), a detailed analysis in an oocyte expression system will be useful as a baseline for future research. In this paper, we present a further characterization of this channel as expressed in *Xenopus* oocytes, focusing on its kinetic properties and the effects of dendrotoxin and charybdotoxin on channel activity.

2. Materials and methods

The cDNA for the rat atrial K^+ channel was obtained from Dr. David Clapham, in the form described in Paulmichl et al. (1991). Capped, poly-adenylated cRNA was synthesized off the SP6 promoter from linearized plasmid using the Megascript kit (Ambion). The product of this reaction was checked for appropriate size by agarose gel electrophoresis and the approximate concentration determined by spectrophotometry. This material was used for injections into oocytes at a concentration of 0.6–0.7 mg/ml.

Adult female *Xenopus laevus* frogs were obtained from Xenopus One (Ann Arbor, MI, USA). Oocytes were collected from anesthetized frogs, which were used once or twice and then euthanized. The ovarian tissue was bluntly dissected, washed in a modified Barth's saline (MBS, in mM: 90 NaCl, 1 KCl, 0.82 $MgCl_2$, 0.74 $CaCl_2$ and 10 Hepes, pH 7.4), then agitated gently for 2 h at room temperature with 250 U/ml collagenase (Gibco) in nominally Ca^{2+}-free MBS, with one solution change. Single defolliculated oocytes were then sorted to obtain the stage-V and -VI cells to be used for injection the following day. Oocytes were injected with 15 ng of cRNA (23 nl) or H_20 using a Drummond Nanoject system, and used for electrophysiological experiments within 2–5 days. Cells were kept in MBS solution with 100 U/ml penicillin and 40 μg/ml gentamicin at 20°C. Recordings were carried out in either MBS or symmetric K^+ solution (in mM, 100 KCl, 0.82 $MgCl_2$, 0.74 $CaCl_2$ and 10 Hepes, pH = 7.4).

Two electrode voltage-clamp experiments were performed at room temperature. Microfilament glass electrodes were pulled to resistances of 0.5–3 MΩ when filled with 0.5 M KCl. Experiments were performed using a Dagan TEV-200 voltage-clamp driven by pClamp software via a Labmaster Tl-1 A/D interface. Low-pass filter cut-off frequency was 200 Hz, sampling intervals were ≤ 2 ms for all except the extended inactivation protocol. Cells were placed in a recording chamber with a 1-ml volume, to which a vacuum drainage tube was attached to facilitate solution changes. Drugs used were obtained from Sigma ($BaCl_2$, CsCl, tetraethylammonium and 4-aminopyridine) or Research Biochemicals (dendrotoxin and charybdotoxin; both recombinant products). Drugs were added via a solution changing apparatus, or directly to the 1-ml chamber, the bath mixed gently by repeated aspiration and allowed to equilibrate for 5 min.

The data obtained from these experiments were analysed using both pClamp (Clampfit) and Axograph software (Axon Instruments). Where data were averaged, values are presented as the mean $\pm$ S.E. In general, representative traces were used for kinetic analysis, after determining 'typical' channel behavior by visual inspection of records. Exponential fits were evaluated by visual inspection of the closeness of fit and the magnitude of the sum of squared errors. For pharmacological experiments, statistical significance was tested using a Student's paired *t*-test on normalized data using each cell as its own control to compensate for variation in the magnitude of expressed currents, or single-factor analysis of variance as indicated in the text.

3. Results

3.1. Channel properties

In a standard step-command voltage protocol, from a holding potential of -80 mV, the rKv1.2 channel is evident as a slowly developing, outwardly rectifying current that shows slow inactivation (Fig. 1A). In a symmetric K^+ solution, large inward currents develop at negative potentials above the activation threshold and large inward tail-currents are seen upon returning the cell to the holding potential (Fig. 1B). In MBS (1 mM external K^+), significant outward current begins to develop above about -25 mV, beyond which the *I–V* curve is roughly linear. In symmetric K^+, it can be seen that a substantial portion of the channels begin to activate near -35 mV. To determine the conductance properties of the open channels in isolation from the effect of voltage-dependent activation, a tail-current protocol was used (Fig. 1C). The resultant *I–V* curve shows that the open-channel conductance is linear over the range of voltages tested.

A steady-state fractional activation curve is presented in Fig. 2A, together with the steady-state inactivation curve.

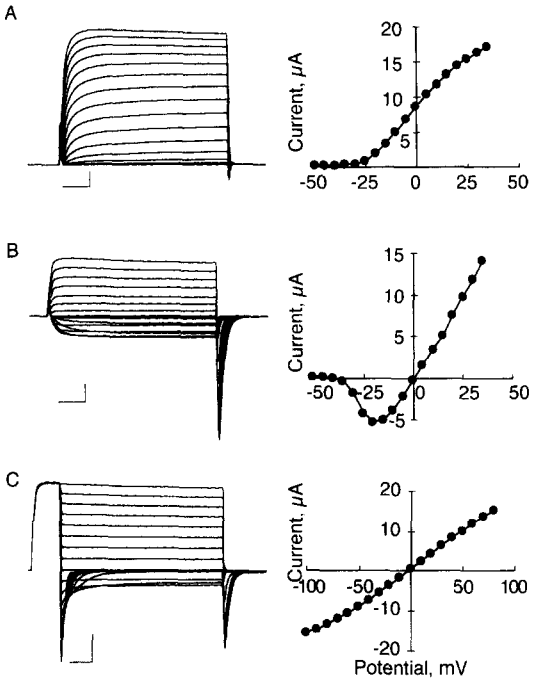

Fig. 1. Representative traces and resultant $I-V$ curves from two different oocytes expressing rKv1.2 using a standard step depolarization protocol in MBS (A) and symmetric K^+ (B). The holding potential in each case was −80 mV and the cells were subjected to a series of step commands from −50 mV through +35 mV in 5 mV increments. For the $I-V$ curves, currents were averaged over the last 50 ms of the step command period. The tail current tracing (C) is from a third representative cell in symmetric K^+ bathing solution. From a holding potential of −80 mV, the cell was stepped to a potential of +80 mV for 50 ms to fully activate the channels then stepped through a series of voltages ranging from −100 mV to +80 mV in 10 mV increments. For the open-channel $I-V$ curve, a single measurement was made 6–8 ms after the end of the activation step to allow for settling of >90% of the capacitance transient. Scale bars: (A) 2 μA, 50 ms; (B) 5 μA, 50 ms; (C) 5 μA, 50 ms.

The tail-currents from the standard step protocol (in symmetric K^+) were measured for each of the command voltages and normalized to the tail-current which followed depolarization to +80 mV. The half-maximal activation voltage ($V_{1/2}$) is approximately −21 mV, with maximal activation occurring near 0 mV. The magnitude of K^+ current was strongly dependent upon the holding potential. Inspection of the current tracings revealed that the rKv1.2 current was virtually eliminated at a holding potential of ≥ 0 mV. Cells were clamped at each tested holding potential for at least 2 min to achieve a new steady-state. From 0 mV, outward currents at 35 mV in injected cells did not differ significantly from those seen in water injected oocytes and were, thus, considered to be solely the result of endogenous channel activity. For each cell, this current was subtracted from the measured current at 35 mV following clamp at each tested holding potential. The resulting difference currents were then normalized and plotted as a function of holding potential. The voltage at which half of the channel population is inactivated is approximately −22 mV.

As with other members of the delayed rectifier class of K^+ channels, the rate of activation of rKv1.2 is voltage-dependent, being significantly slower at less depolarized voltages. For comparison, our measurements of the kinetics of activation were similar to those previously reported, with mean time constants of 37 ± 7 ms at −30 mV and 7 ± 1 ms at 35 mV ($n = 5$ cells). The relationship of the deactivation time constant (τ_d) to membrane voltage is shown in Fig. 2B. Data are obtained by fitting a curve to the tail-currents following settling of 95% of the membrane capacitance transient (the time constant of which was typically 1–2 ms). In all cases, the remainder of the tail-current was very well fit by a single exponential equation. The rate of deactivation slows significantly as the cell is returned to less negative voltages. Above −40 mV it becomes difficult to identify a meaningful deactiva-

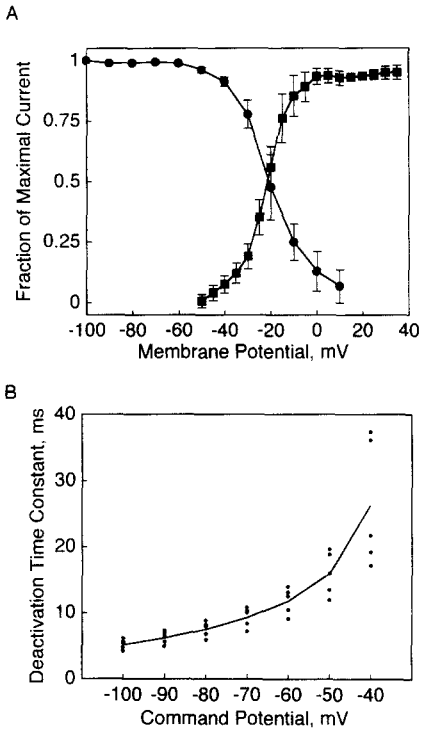

Fig. 2. (A) Steady-state inactivation and fractional activation curves. Steady-state inactivation (●) was determined by stepping to +35 mV following 2 min at each holding potential and normalizing relative to the currents obtained from a holding potential of −100 mV. Virtually complete inactivation of this K^+ channel occurs at a holding potential of 0 mV. The fractional activation curve (■) was generated by measuring the magnitude of the tail current at −80 and plotting that value as a function of the previous command voltage, normalized with respect to the tail current occuring after depolarization to +80mV. Points are mean ± S.E. values from 3–8 cells for the steady-state inactivation curve, 4 cells for the fractional activation curve. (B) The relationship of the deactivation kinetics to the membrane potential. The time point chosen for the beginning of the exponential fit for all tracings is determined by identifying the 'end' of the transient in the step to −20 mV (see Fig. 1c), 6–8 ms after the voltage step. A single exponential equation described the remainder of the tail current very well. Individual points at each voltage are from different cells ($n = 5$) and the solid line represents the mean τ value.

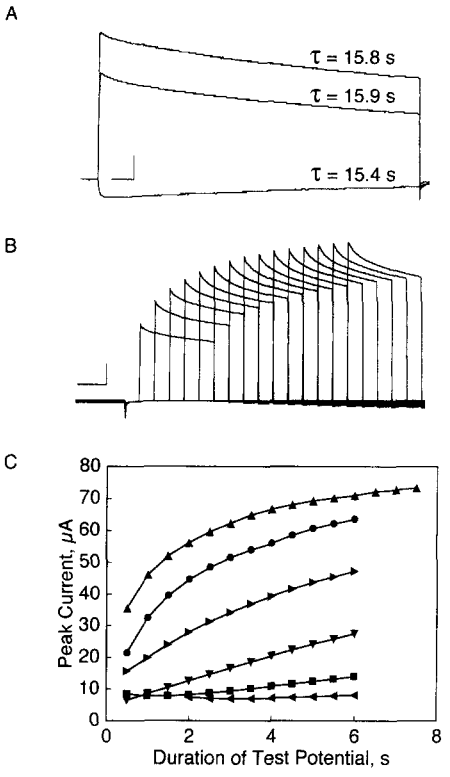

Fig. 3. Kinetics of inactivation. The current trace (A) shows an example of the current during a long activation protocol. Only three of the traces are shown here for clarity: −20, 40 and 60 mV (scale bars: 1 μA, 1 s). A double-exponential equation provided the best fit. The holding potential was −80 and, after each episode, the cell was clamped to the holding potential for 5 s to allow recovery from inactivation prior to the next voltage step. The second time constant is indicated for each of these traces. Neither time constant could be correlated with membrane potential. Recovery from inactivation was voltage-dependent (B). A representative family of currents from the protocol designed to measure the rate of recovery is shown (scale bars: 10 μA, 1 s). The cell is first held at 0 mV for 2 min to fully inactivate rKv1.2. Following periods of increasing duration at a test potential (−80 mV in this example), the cell is depolarized to +80 mV and the peak current used to determine the extent of recovery from inactivation. This protocol was carried out using different test potentials ranging from −80 mV to −30 mV, as shown from a representative cell in C. At no voltage was there measurable inward current, consistent with full inactivation of rKv1.2. Over the range of voltages tested, recovery is most rapid at −80 mV and does not occur above about −40 mV. ▲, −80 mV; ●, −70 mV; ►, −60 mV; ▼, −50 mV; ■, −40 mV; and ◄, −30 mV.

tion time constant as the current change reflects simply the change in driving force, with little evidence that a significant number of channels actually close.

Like many other delayed rectifier K^+ channels, this Kv1.2 channel undergoes slow inactivation following activation. Fig. 3A shows three voltage steps from a representative cell using an extended protocol designed to study the kinetics of inactivation of the rKv1.2 channel. A double exponential equation was fit to the traces at voltages where significant inward or outward currents develop. For consistency, the starting time point for the fit was the point of peak outward current at the most depolarized voltage; even for inward currents in which the peak current occurred significantly later the inactivation component was well described using the earlier time point. Neither time constant was consistently affected by voltage. From a group of 8 cells, the first (minor) time constant averaged 0.5 s (S.E. = ±0.1 s). The mean second time constant was 13.9 s (S.E. = ±0.9 s).

The dependence of current magnitude on holding potential suggests that inactivation may accumulate at moderate depolarizations. To characterize the process of recovery from inactivation, cells were clamped at zero to fully inactivate the rKv1.2 channels. They were then stepped to a test potential (−80 to −30 mV) for increasing lengths of time, after which they were stepped to +80 mV to determine the maximal available current (Fig. 3B). The absence of a steady-state or tail-current upon stepping to the test potential indicates that the channels are fully inactivated at the holding potential and that they do not open to any significant degree during the test period. Thus, the outward current upon depolarization reflects the extent to which the channels have moved from the inactivated state to the closed but available state. Fig. 3C shows the results of a series of these protocols from a single cell, with the peak current measurements plotted against the duration of the test potential step. Recovery from inactivation is significantly more rapid at strongly hyperpolarized membrane potentials and virtually eliminated above −40 mV.

3.2. Pharmacology

Several commonly used K^+ channel blockers were used to characterize rKv1.2 pharmacologically. Results with Ba^{2+}, 4-aminopyridine and tetraethylammonium were consistent with those reported previously for this channel. In addition, we observed that 5 mM Ba^{2+} completely blocked inward current in symmetric K^+ solution and extracellular cesium (5 mM) had no effect on inward or outward current (data not shown). Fig. 4 shows representative tracings and a concentration-response curve for dendrotoxin. To determine whether there was voltage dependency of dendrotoxin block, we compared concentration-response curves from currents at −20 mV (inward in symmetric K^+ solution) to those at +35 mV (outward currents). Data from each of 5 cells were analyzed as in Fig. 4B, and curves fitted by a least-squares method to a general equation which describes a sigmoidal curve: $R = [D]^n/([D]^n + K^n)$, where R is the fraction of maximal response and K^n and n are fitting parameters (Kenakin, 1987). K^n provides a measure of the IC_{50} and, in this case, n is constrained to one in view of the simple bimolecular kinetics of binding. Mean IC_{50} values were 2.8 ± 0.52 nM for inward current and 8.6 ± 3.7 nM for outward current ($P = 0.07$, one-tailed t-test); there appears to be a trend toward greater sensitivity for inward current. Dendrotoxin had no effect on the activation kinetics of this channel. For a step to +40 mV, the 95% rise times were 26.4 ± 2.4 and

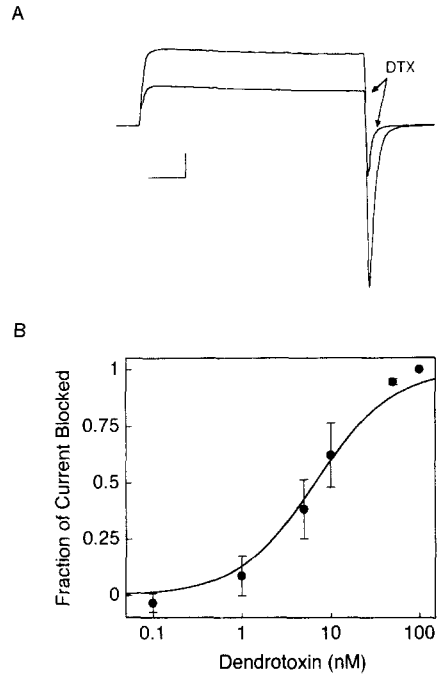

Fig. 4. rKv1.2 is sensitive to block by the snake venom toxin α-dendrotoxin at nanomolar concentrations. As shown in A by the superimposed traces from the same cell before and after addition of 10 nM α-dendrotoxin, extracellular dendrotoxin reduced the magnitude of current without appreciably affecting kinetics (symmetric K^+ bathing solution, command potential = 35 mV, scale bar: 5 μA, 50 ms). The dose-response curve at +35 mV is shown in B as mean ± S.E. ($n = 5$ cells). Maximal response was considered to have been achieved with 100 nM dendrotoxin, at which point inward currents were absent and outward currents were not significantly different from water-injected oocytes (not shown), indicating virtually complete block of rKv1.2 current.

25.9 ± 1.4 ms for control and 50 nM dendrotoxin conditions, respectively (mean ± S.E., $n = 5$ cells).

Charybdotoxin blocks this channel at concentrations similar to those seen with dendrotoxin. The effect of charybdotoxin on the macroscopic current is quite different than that of dendrotoxin, although the toxins share similar architecture (Schweitz et al., 1989). Fig. 5A,B shows current tracings from a cell in the presence of 0 or 50 nM charybdotoxin. The charybdotoxin effect is completely reversible; a trace following washout of 100 nM charybdotoxin is virtually indistinguishable from the pre-treatment control (data not shown). The initial reduction in current magnitude is consistent with a significant degree of toxin binding prior to channel activation. This process is well fit by a single exponential, with a mean τ value of 86 ms. Fig. 5C shows the steady-state concentration-response curve for charybdotoxin at 35 mV. The mean IC_{50} was 5.6 ± 1.8 nM, $n = 6$ cells; there was less than 1 nM difference between the IC_{50} values for inward and outward current when analyzed as described above for dendrotoxin.

Charybdotoxin in the bathing solution altered the deactivation kinetics of this K^+ current. The tail-current protocol presented in Fig. 6A shows that the time constants for deactivation are significantly shorter in the presence of charybdotoxin (50 nM) compared to control conditions (see Fig. 1); this can also be seen in the tracings in Fig. 5. At higher concentrations, charybdotoxin blocked the current to the extent that what little deactivation current remained is obscured by the capacitance transient. However, under conditions of partial block, it is possible to estimate the deactivation time constant. Fig. 6B shows the deactivation time constants at various voltages as affected by charybdotoxin. As charybdotoxin concentration increases, there is a concomitant reduction in τ_d at all voltages tested. This effect was not observed for concentrations of dendrotoxin producing comparable reductions in current magnitude; for example, the time constants for deactivation at −80 mV were 5.4 ± 1.1 and 4.1 ± 1.0 ms in 5 and 50 nM dendrotoxin, respectively ($n = 3$ cells). These values are not significantly different from each other or from τ_d in the absence of dendrotoxin (using single-factor analysis of variance).

As part of the characterization of charybdotoxin interactions with rKv1.2, we investigated the process of recovery

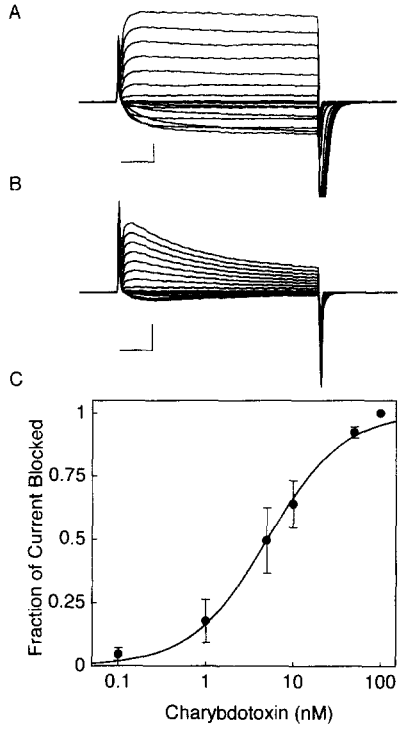

Fig. 5. Effect of charybdotoxin of rKv1.2 current. The standard step protocol was used to generate the representative current families from 1 cell shown in A and B, control or 50 nM charybdotoxin respectively (scale bars: 2 μA, 50 ms; truncation of the tail current in A is due to saturation of the amplifier). An indication of the kinetics of binding to the open channels was obtained by fitting the current decay to a single exponential equation starting from the point of peak current amplitude, yielding a mean time constant of 86 ms ± 9.4 ms, $n = 6$ cells, measured at 35 mV). Cumulative dose-response curve for charybdotoxin at 35 mV is shown in C. As with dendrotoxin, steatdy-state current in the presence of 100 nM charybdotoxin was not significantly different than endogenous currents. Currents were averaged over the last 50 ms of the depolarization steps and normalized for each cell to currents obtained in the absence of charybdotoxin. Data are shown as the means ± S.E. at each dose from 4–7 different cells.

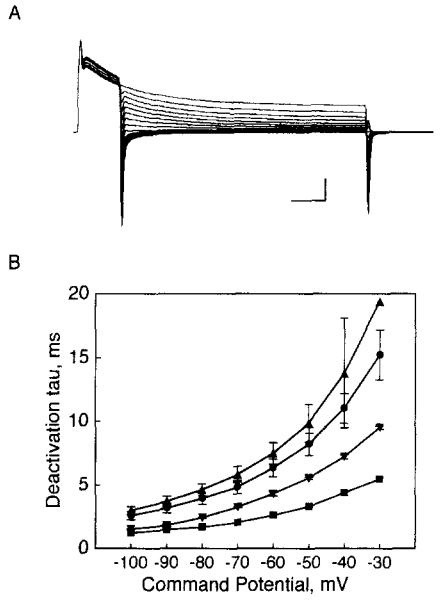

Fig. 6. Effect of charybdotoxin on rKv1.2 deactivation. A representative tracing using the tail current protocol in symmetric K^+ bathing solution in the presence of 50 nM charybdotoxin is shown in A (scale bars: 2 μA, 50 ms). Note the very rapid deactivation at less depolarized voltages compared to the tracing shown in Fig. 1C. Time constants for the deactivation process were determined as described in the text using a single exponential equation from 7 cells at 0 nM, 4 at 10 nM, 3 at 50 nM charybdotoxin and 1 cell at 100 nM. The mean τ values ± S.E. at the following concentrations are plotted in B: ▲, control; ●, 10 nM; ▼, 50 nM; and ■, 100 nM.

from the activation-dependent phase of block. From the tail-current experiments performed in the presence of charybdotoxin, it could be seen that the extent of channel inhibition reached a steady-state level over the course of the 400-ms voltage command period, but then returned to the level at which it had been before the first episode

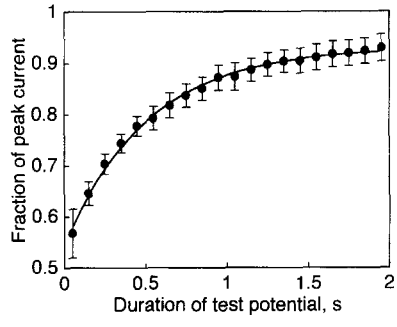

Fig. 7. Recovery from open-channel phase of charybdotoxin block. A double-pulse protocol was used to determine the kinetics of this process. An initial depolarization step (1.3 s) was used to activate the channel and approach a steady-state of accumulated block by charybdotoxin while inducing a minimal degree of intrinsic inactivation. A hyperpolarizing step of increasing duration closed the channels and the second depolarizing step reveals the extent to which open-channel charybdotoxin block was relieved during the period of channel closure. The peak currents from the second depolarization are expressed as a fraction of the peak from the corresponding first depolarization and plotted against the length of the hyperpolarization step. Data are shown as mean ± S.E. values for $n = 5$ cells; the solid line is the fitted curve using a single exponential equation with a time constant of 0.51 s.

within the approximately one second between episodes (holding potential = −80 mV). To characterize the kinetics of toxin dissociation, we used a two-step protocol similar to that which has been used for determination of recovery from inactivation of sodium channels (for a review, see Hille, 1992). As with recovery from inactivation, a time constant for the recovery from charybdotoxin block was determined by measuring the peak current after a test period at various membrane potentials. These currents were normalized by episode to the peak current during the pre-pulse, plotted vs. duration of the test potential step and then fit to a single exponential equation (Fig. 7). The mean time constant for the recovery process at −80 mV was 0.5 ± 0.1 s ($n = 4$). There was no correlation between the time constant for recovery from charybdotoxin block and test potential. These data are consistent with the existence of different binding equilibria for open and closed channels.

4. Discussion

In this paper, we have extended the kinetic and pharmacologic characterization of a rat Kv1.2 channel. The behavior of this channel in our system was comparable to the initial characterization (Paulmichl et al., 1991) with respect to the *I–V* relation and voltage dependence and kinetics of activation. Data presented here show the $V_{1/2}$ for activation and the $V_{1/2}$ for steady-state inactivation to be very similar (−21 mV and −22 mV, respectively). Between −40 mV and 0 mV, there is a significant open probability for this channel, consistent with a role in membrane repolarization following an action potential. As with activation, the deactivation process is voltage-dependent, exhibiting a 5-fold increase in the time-constant between −100 mV and −40 mV. Time constants for inactivation were not voltage-dependent.

Inward currents through the rKv1.2 channel were blocked by Ba^{2+}, but not cesium or tetraethylammonium. Outward currents were not significantly inhibited by any of these compounds at the concentrations tested (5 mM Ba, Cs; 10 mM tetraethylammonium); Paulmichl et al. (1991) reported about 50% block by 10 mM extracellular Ba^{2+}. The lack of sensitivity to extracellular tetraethylammonium is consistent with what is known about the structural features of K^+ channels that contribute to tetraethylammonium affinity. In particular, the amino acid at the position equivalent to residue 381 in rKv1.2 has been shown to strongly affect tetraethylammonium affinity (MacKinnon and Yellen, 1990; Kavanaugh et al., 1991, 1992) through a predominantly hydrophobic rather that electrostatic interaction (Taglialatela et al., 1991; Armstrong and Hille, 1972; Mozhayeva and Naumov, 1972; Christie et al., 1990; Spruce et al., 1987). K^+ channels with an aromatic residue at this position generally are sensitive to external tetraethylammonium block (EC_{50} values of less than 1 mM) while other hydrophobic residues

at this position are associated with moderate to low sensitivity and positively charged residues confer virtually complete resistance to tetraethylammonium block. rKv1.2 has a valine residue at this position; two very closely related voltage-gated K^+ channels from rat ventricle and brain with valine at this site were reported to have EC_{50} values for tetraethylammonium greater than 100 mM (Stühmer et al., 1989; Christie et al., 1990).

The venom toxins charybdotoxin and dendrotoxin both block this K^+ channel with high affinity, although the kinetics of block are distinct. Dendrotoxin reduces the magnitude of the current without affecting the time constants for activation or deactivation over a range of voltages from −100 mV to +80 mV. This is not true for all types of K^+ channels; dendrotoxin has been shown to significantly prolong the deactivation process in at least one other delayed rectifier (Sprunger and O'Grady, 1996). In contrast, charybdotoxin produces a marked change in the kinetics of the macroscopic current, with the evoked current decaying more rapidly in the presence of charybdotoxin. While it is possible that charybdotoxin binds only after activation and the reduction in initial current magnitude is actually the result of rapid onset of block, this would be inconsistent with other studies of charybdotoxin effects on Ca^{2+}- and voltage-activated K^+ channels, which have not shown block to be activation-dependent. It is more likely that the smaller magnitude of the initial current in the presence of charybdotoxin indicates that channel opening is not required for toxin binding, and the accelerated current decay following activation reflects further accumulation of binding and block of open channels by the toxin. The intrinsic channel inactivation underlies this process, but the predominant time constant for channel inactivation is nearly 200 times that of the charybdotoxin effect, so the contribution over the course of a 300-ms voltage step would be minimal. The recovery from the open-channel phase of charybdotoxin block is much faster than recovery from inactivation (cf., Fig. 3C, Fig. 7), further distinguishing accumulation of charybdotoxin block and intrinsic channel inactivation.

An interesting comparison may be drawn between the effect of charybdotoxin on a delayed rectifier as described here, and its effect on Ca^{2+}-activated maxi-K^+ channels. A recent paper showed *hslo* from vascular smooth-muscle cells to be sensitive to charybdotoxin, but with no effect on the macroscopic current kinetics (McCobb et al., 1995). However, an earlier single-channel study of a large conductance Ca^{2+}-activated K^+ channel reconstituted into a phospholipid bilayer showed convincingly that, while charybdotoxin could bind to both open and closed channels, the rate of association was approximately 7-fold greater for open vs. closed channels. The determinants of the relative affinities for open and closed channels remain to be identified, but it is reasonable to speculate that three-dimensional changes in the outer vestibule upon channel activation could alter toxin affinity. The particular residues present in the S5-S6 linker, which also determine pre-activation toxin binding, may well determine whether a specific channel exhibits the additional open-channel sensitivity observed with this Kv1.2 channel.

Of particular interest in this study is the effect of charybdotoxin on the deactivation kinetics of this Kv1.2 current. The most straightforward interpretation would be a mechanism involving voltage-dependent block of charybdotoxin such that toxin binding is enhanced at more negative voltages as a direct effect of the membrane electric field on the charged toxin molecule. Reports of voltage dependency of charybdotoxin block vary; in addition to a voltage-dependent interaction (Goldstein and Miller, 1993), a voltage-independent interaction has also been described (Jacobs and DeCoursey, 1990). Between +35 and −20 mV, we saw no change in the steady-state concentration-response curve, so the data in this study do not support voltage-dependent charybdotoxin block over that voltage range. However, the question of voltage dependency of charybdotoxin binding remains open, since the effect on deactivation occurs at voltages more negative than the activation threshold and a non-linear effect of voltage cannot be ruled out.

In the absence of a direct effect of membrane voltage on the toxin itself, the deactivation effect may reflect changes in state transitions of the channel. One possibility is that the deactivation process per se is facilitated by a non-blocking state of charybdotoxin interaction with an open channel, a type of interaction which would not otherwise be apparent in an electrophysiological analysis. We are not aware of any other studies which could provide support for such an interaction. Alternatively, charybdotoxin could change one or more closed-to-open transition rate constants in addition to blocking the pore. Differential effects on deactivation and activation suggest the events are not simply the same process in reverse. This is consistent with a recent in-depth study of Shaker channel gating, in which evidence was presented for the existence of at least two closed states which the channel may enter after opening which are not in the activation pathway, in addition the activation pathway closed state(s) to which the open channel may return (Hoshi et al., 1994; Zagotta et al., 1994a,b). The stabilization of a repolarization-induced closed state, particularly one that would be short-lived in the absence of charybdotoxin, could have the effect on macroscopic current observed here. Binding of charybdotoxin in the first few ms after repolarization would reduce the probablility of the channel returning to the open state, resulting in a shortened ensemble mean tail-current.

Recent work involving site-directed mutagenesis and charybdotoxin analogs has been quite informative with regard to the structure of the outer mouth of the pore. The present results suggest that a similar experimental approach in conjuction with single-channel analysis may also prove useful in the analysis of structural components involved in the process of voltage-gated K^+ channel deacti-

vation. Furthermore, it will be of interest to determine how deactivation of other types of K^+ channels is affected by members of this class of peptide toxins. Identification of naturally occurring ionic currents in intact cells with cloned channels is not always straightforward. Specific toxin effects, such as the deactivation rate change described here, may prove useful as molecular tags to determine contribution to cellular currents of particular channel subtypes.

Acknowledgements

L.K.S. was a Howard Hughes Medical Institute Predoctoral Fellow during the time that part of this study was done. Additional support was provided by a grant to L.K.S. from NHLBI and a MN AES grant to S.M.O.

References

Andersen, O.S. and R.E. Koeppe, 1992, Molecular determinants of channel function, Physiol. Rev. 72 (Suppl.), S89.

Armstrong, C.M. and B. Hille, 1972, The inner quaternary ammonium ion receptor in potassium channels of the node of Ranvier, J. Gen. Physiol. 59, 338.

Brent, L.H., J.L. Butler, W.T. Woods, Jr. and J.K. Bubien, 1990, Transmembrane ion conductance in human B lymphocyte activation, J. Immunol. 145, 2381.

Brown, A.M., 1993, Functional bases for interpreting amino acid sequences of voltage-dependent K channels, Annu. Rev. Biophys. Biomol. Struct. 22, 173.

Chandy, K.G., 1991, Simplified gene nomenclature, Nature 352, 26.

Christie, M.J., R.A. North, P.B. Osborne, J. Douglass and J.P. Adelman, 1990, Heteropolymeric potassium channels expressed in *Xenopus* oocytes from cloned subunits, Neuron 2, 405.

Cooper, K., P. Gates, J.L. Rae and J. Dewey, 1990, Electrophysiology of cultured human lens epithelial cells, J. Membr. Biol. 117, 285.

Giangiacomo, K.M., M.L. Garcia and O.B. McManus, 1992, Mechanism of iberiotoxin block of the large-conduction calcium-activated potassium channel, Biochemistry 31, 6719.

Goldstein, S.A.N. and C. Miller, 1992, A point mutation in a *Shaker* K channel changes its charybdotoxin binding site from low to high affinity, Biophys. J. 62, 5.

Goldstein, S.A.N. and C. Miller, 1993, Mechanism of charybdotoxin block of a voltage-gated K channel, Biophys. J. 65, 1613.

Goldstein, S.A.N., D.J. Pheasant and C. Miller, 1994, The charybdotoxin receptor of a Shaker K channel: peptide and channel residues mediating molecular recognition, Neuron 12, 1377.

Grissmer, S., A.N. Nguyen, J. Aiyar, D.C. Hanson, R.J. Mather, G.A. Gutman, M.J. Karmilowicz, D.D. Auperin and K.G. Chandy, 1994, Pharmacological characterization of five cloned voltage-gated K Channels, types Kv1.1, 1.2, 1.3, 1.5, and 3.1 stably expressed in mammalian cell lines, Mol. Pharmacol. 45, 1227.

Gross, A., T. Abramson and R. MacKinnon, 1994, Transfer of the scorpion toxin receptor to an insensitive potassium channel, Neuron 13, 961.

Hille, B., 1992, Ionic Channels of Excitable Membranes (Sinauer, Sunderland, MA).

Hoshi, T., W.N. Zagotta and R.W. Aldrich, 1994, Shaker potassium channel gating I: transitions near the open state, J. Gen. Physiol. 103, 249.

Jacobs, E.R. and T.E. DeCoursey, 1990, Mechanisms of potassium channel block in rat alveolar epithelial cells, J. Pharmacol. Exp. Ther. 255, 459.

Katz, A.M., 1993, Cardiac ion channels, N. Engl. J. Med. 328, 1244.

Kavanaugh, M.P., M.D. Varnum, P.B. Osborne, M.J. Christie, A.E. Busch, J.P. Adelman and R.A. North, 1991, Interaction between tetraethylammonium and amino acid residues in the pore of cloned voltage-dependent potassium channels, J. Biol. Chem. 166, 7583.

Kavanaugh, M.P., R.S. Hurst, J. Yakel, M.D. Varnum, J.P. Adelman and R.A. North, 1992, Multiple subunits of a voltage-dependent potassium channel contribute to the binding site for tetraethylammonium, Neuron 8, 493.

Kenakin, T.P., 1987, Pharmacologic Analysis of Drug-Receptor Interaction (Raven, New York, NY).

Leonard, R.J., M.L. Garcia, R.S. Slaughter and J.P. Reuben, 1992, Selective blockers of voltage-gated K channels depolarize human T lymphocytes: mechanism of the antiproliferative effect of charybdotoxin, Proc. Natl. Acad. Sci. USA 89, 10094.

MacKinnon, R. and C. Miller, 1988, Mechanism of charybdotoxin block of the high-conduction, Ca^{2+}-activated K^+ channel, J. Gen. Physiol. 91, 335.

MacKinnon, R. and G. Yellen, 1990, Mutations affecting TEA blockade and ion permeation in voltage-activated K channels, Science 250, 176.

McCobb, D.P., N.L. Fowler, T. Featherstone, C.J. Lingle, M. Saito, J.E. Krause and L. Salkoff, 1995, A human calcium-activated potassium channel gene expressed in vascular smooth muscle, Am. J. Physiol. 269, H767.

Miller, C., 1988, Competition for block of a Ca2+-activated K+ channel by charybdotoxin and tetraethylammonium, Neuron 1, 1003.

Mozhayeva, B.N. and A.P. Naumov, 1972, Tetraethylammonium ion inhibition of potassium conductance of the nodal membrane, Biochim. Biophys. Acta 290, 248.

O'Grady, S.M., K.E. Cooper and J.L. Rae, 1991, Cyclic GMP regulation of a voltage-activated K channel in dissociated enterocytes, J. Membr. Biol. 124, 159.

Paulmichl, M., P. Nasmith, R. Hellmiss, K. Reed, W.A. Boyle, J.M. Nerbonne, E.G. Peralta and D.E. Clapham, 1991, Cloning and expression of a rat cardiac delayed rectifier potassium channel, Proc. Natl. Acad. Sci. USA 88, 7892.

Pongs, O., 1992, Molecular biology of voltage-dependent potassium channels, Physiol. Rev. 72, S69.

Pongs, O., 1993, Structure-function studies on the pore of potassium channels, J. Membr. Biol. 136, 1.

Schweitz, H., J.-N. Bidard, P. Maes and M. Lazdunski, 1989, Charybdotoxin is a new member of the K channel toxin family that includes dendrotoxin I and mast cell degranulating peptide, Biochemistry 28, 9708.

Spruce, A.E., N.B. Standen and P.R. Stanfield, 1987, The action of tetraethylammonium ions on unitary delayed rectifier potassium channels of frog skeletal muscle, J. Physiol. 393, 467.

Sprunger, L.K. and S.M. O'Grady, 1996, Properties of a delayed-rectifier K^+ channel in a mouse nonfusing muscle cell line, Cell. Physiol. Biochem., in press.

Stühmer, W., J.P. Ruppersberg, K.H. Schröter, B. Sakmann, M. Stocker, K.P. Giese, A. Perschke, A. Baumann and O. Pongs, 1989, Molecular basis of functional diversity of voltage-gated potassium channels in mammalian brain, EMBO J. 8, 3235.

Taglialatela, M., A.M.J. VanDongen, J.A. Drewe, R.H. Joho, A.M. Brown and G.E. Kirsch, 1991, Patterns of internal and external tetraethylammonium block in four homologous K channels, Mol. Pharmacol. 40, 299.

Verheugen, J.A.H., M. Oortgiesen and H.P.M. Vijverberg, 1994, Veratridine blocks voltage-gated potassium current in human T lymphocytes and in mouse neuroblastoma cells, J. Membr. Biol. 137, 205.

Zagotta, W.N., T. Hoshi and R.W. Aldrich, 1994a, Shaker potassium channels III: evaluation of kinetic models for activation, J. Gen. Physiol. 103, 321.

Zagotta, W.N., T. Hoshi, J. Dittman and R.W. Aldrich, 1994b, Shaker potassium channel gating II: transitions in the activation pathway, J. Gen. Physiol. 103, 279.